tvst

Retina

Effects of Different Spectrum of LEDs on Retinal Degeneration Through Regulating Endoplasmic Reticulum Stress

Wenyi Chen[1,2], Rong Lin[1,2], Kunhong Xiao[1], Kun Yuan[3], Zhongjiang Chen[1], and Yan Huang[1]

[1] Department of Ophthalmology and Optometry, Fujian Medical University, Fuzhou, China
[2] Medical Technology Experimental Teaching Center, Fujian Medical University, Fuzhou, China
[3] Fuwai Hospital, Peking Union Medical College, Beijing, China

Correspondence: Yan Huang, Department of Ophthalmology and Optometry, Fujian Medical University, Fuzhou 350004, Fujian Province, China. e-mails: fjhyan-1988@fjmu.edu.cn, 13960888823@139.com

Received: September 26, 2022
Accepted: February 21, 2023
Published: June 26, 2023

Keywords: full-spectrum LED; spectral distribution; S-opsin; retinal degeneration; ER stress

Citation: Chen W, Lin R, Xiao K, Yuan K, Chen Z, Huang Y. Effects of different spectrum of LEDs on retinal degeneration through regulating endoplasmic reticulum stress. Transl Vis Sci Technol. 2023;12(6):16, https://doi.org/10.1167/tvst.12.6.16

Purpose: To evaluate the impact of full-spectrum light-emitting diodes (LEDs) on albino guinea pigs' retina and investigate the roles of short-wavelength opsin (S-opsin) and endoplasmic reticulum (ER) stress in light-induced retinal degeneration (LIRD).

Methods: Three-week-old albino guinea pigs ($n = 30$) were distributed into five groups under 12/12 light/dark cycles with indoor natural light (NC; 300–500 lux, $n = 6$), full-spectrum LEDs (FL; 300 lux, $n = 6$; 3000 lux, $n = 6$), and commercial cold-white LEDs (CL; 300 lux, $n = 6$; 3000 lux, $n = 6$) and raised for 28 days. Hematoxylin and eosin staining and transmission electron microscopy evaluated the morphological changes of retinas. The immunofluorescence and real-time quantitative polymerase chain reaction (RT-qPCR) measured the expression and content of S-opsin and ER stress-related genes and proteins.

Results: We found that albino guinea pigs exposed to FL at either 300 lux or 3000 lux developed less severe retinal morphological damage than animals exposed to the CL light, which emerged as a significant characteristic of LIRD. Meanwhile, the damage on the ventral retina was more serious, mainly due to its ability to absorb the blue light in the LEDs more easily. Compared to the FL-exposed groups, the CL light increased the aggregation of S-opsin and the expression of ER stress-related factors.

Conclusions: Commercial cold-white LEDs can induce ER stress and unfolded protein response in LIRD, and full-spectrum LED attenuates LIRD by regulating ER stress in albino guinea pig retinas in vivo.

Translational Relevance: Full-spectrum LEDs offer specific eye protection and eye adaptability that can well replace commercial cold-white LEDs in both clinical practice and research. It should be further developed for lighting used in health care facilities.

Introduction

Sunlight has a full spectrum that includes wavelengths ranging from approximately 300 nm to approximately 1200 nm, and the light intensity distribution of various colors is average and soft.[1] Sunlight is essential for development of the eye.[2] It has been suggested that outdoor sunlight exposure is considered a protective behavior in myopia prevalence and progression.[3] However, commercial cold-white light-emitting diodes (LEDs) are still commonly used as indoor lighting in clinical care and animal experiments.[4] Though it has a solid spectral continuity (400–700 nm), its energy is not uniform, and the energy of the blue wavelength (400–500 nm) is still the highest.[5]

Blue LED light is associated with visual fatigue, dry eye, color blindness, myopia, photoreceptor degeneration, light-induced retinal degeneration (LIRD), and so on.[6–8] LIRD is a model that resembles human retinal degenerative diseases, and its main

hallmarks are similar to those detected in age-related macular degeneration, juvenile macular degeneration, or retinitis pigmentosa, which mainly injure the outer retina.[9,10]

It was found that LIRD is related to endoplasmic reticulum (ER) stress, which has often been studied in neurodegenerative diseases, including Alzheimer's disease, Parkinson's disease, and so on.[11] Ooe et al.[12] reported that blue LED light caused aggregation of short-wavelength opsin (S-opsin) and induced ER stress. Another study[13] also found that bilberry extract and anthocyanins can suppress the aggregation of S-opsin induced by exposure to blue LED light in the photoreceptor cell line and reduce ER stress to inhibit LIRD. These findings suggest that ER stress may be a mechanism of LIRD.

The lighting industry today uses sunlight as a benchmark to evaluate the quality of light sources.[14] In order to simulate natural sunlight, full-spectrum LEDs available on the market enhance spectral continuity and integrity; most importantly, they increase the peak value of the green wavelength and red wavelength (500–700 nm) in light intensity, resulting in higher uniformity of colors,[15,16] which also increases the color rendering index of light.[17] Najjar et al.[18] observed that the spectral content of ambient white light is related to ocular growth, and the importance of the spectrum of light on ocular growth and myopia development has been demonstrated in several animal models.[19,20] Previously, we reported that full-spectrum LEDs could attenuate the pathological injury of the lacrimal gland and retina of rats.[21] Krigel et al.[22] reported differences in LIRD with different light sources, protocols, and species of animals. Here, we studied the different effects of retinal degeneration induced by full-spectrum LEDs and commercial cold-white LEDs in albino guinea pigs, and we further explored whether the damage is related to endoplasmic reticulum stress.

Methods

Animal

This study used a total of 30 healthy male albino guinea pigs that were 3 weeks old (Shanghai SLAC Laboratory Animal Center, Shanghai, China). All animal experiments were approved by an animal experiment ethics audit of Fujian Medical University and complied with the ARVO Statement for the Use of Animals in Ophthalmic and Vision Research. The albino guinea pigs were reared under a climate-controlled condition on a 12/12-hour light/dark cycle.

LED Exposure

The albino guinea pigs were divided into a control group of animals living in the indoor natural light (NC group: 300–500 lux, $n = 6$); two groups of animals exposed to full-spectrum LED lights that simulate sunlight with illuminances of 300 lux and 3000 lux (Ra 95 luminance; FL-300 group, $n = 6$; FL-3000 group, $n = 6$; Sungoing Optoelectronics Technology Co., Ltd., Quanzhou, China[23]); or two groups of animals exposed to commercial cold-white LEDs with 300 lux and 3000 lux intensities (Ra 83 luminance; CL-300 group, $n = 6$; CL-3000 group, $n = 6$). Ambient light levels were measured at the animals' eye position using a spectrometer (HOPOO Light & Color Technology Co., Ltd., Hangzhou, China). Before the experiment, all animals were adapted to the dark for 2 days. The lighting houses were custom-made breeding cages with LED panels on the ceilings. The outer periphery and bottom of the cell were covered with a light-reflecting cloth to ensure uniform light in the cage and protect the animals from the light present in the room (Fig. 1). Except for the NC group, the animals were housed under LEDs for 12 hours every day from 6:00 AM to 6:00 PM with food and water. For the remaining 12 hours, all animals were kept in the dark, continuing for 28 days. To allow conditions to be as close to domestic lighting as possible, the pupils were not dilated, like animals in other light models.[24]

Hematoxylin and Eosin Staining

Retinas were collected under the assigned illuminance level for each animal after 28 days; at least three animals were used per exposure condition. Hematoxylin and eosin (H&E) staining and transmission electron microscope were applied to characterize the retinal structure, and immunofluorescence staining observed the expression and location of S-opsin and glucose-regulated protein 78 (GRP78/Bip) proteins.

For histology, the albino guinea pigs were euthanized for tissue preparation. The eyes were enucleated and fixed in Fas eyeball fixation solution (Wuhan Servicebio Technology Co., Ltd., Wuhan, China) for 72 hours, then dehydrated with gradient alcohol, transparent xylene, and paraffin embedding. Finally, a 4-µm-thick tissue specimen was obtained using a paraffin slicer for H&E staining. Observation and collection of images were performed using a 400× optical microscope (Nikon Eclipse E100; Nikon Instruments, Tokyo, Japan). Photographs were taken at equal retinal eccentricities from the optic nerve head. The thickness of the photoreceptor layer was measured from the external limiting membrane to the upper retinal pigment epithelium (RPE) border using the CaseViewer

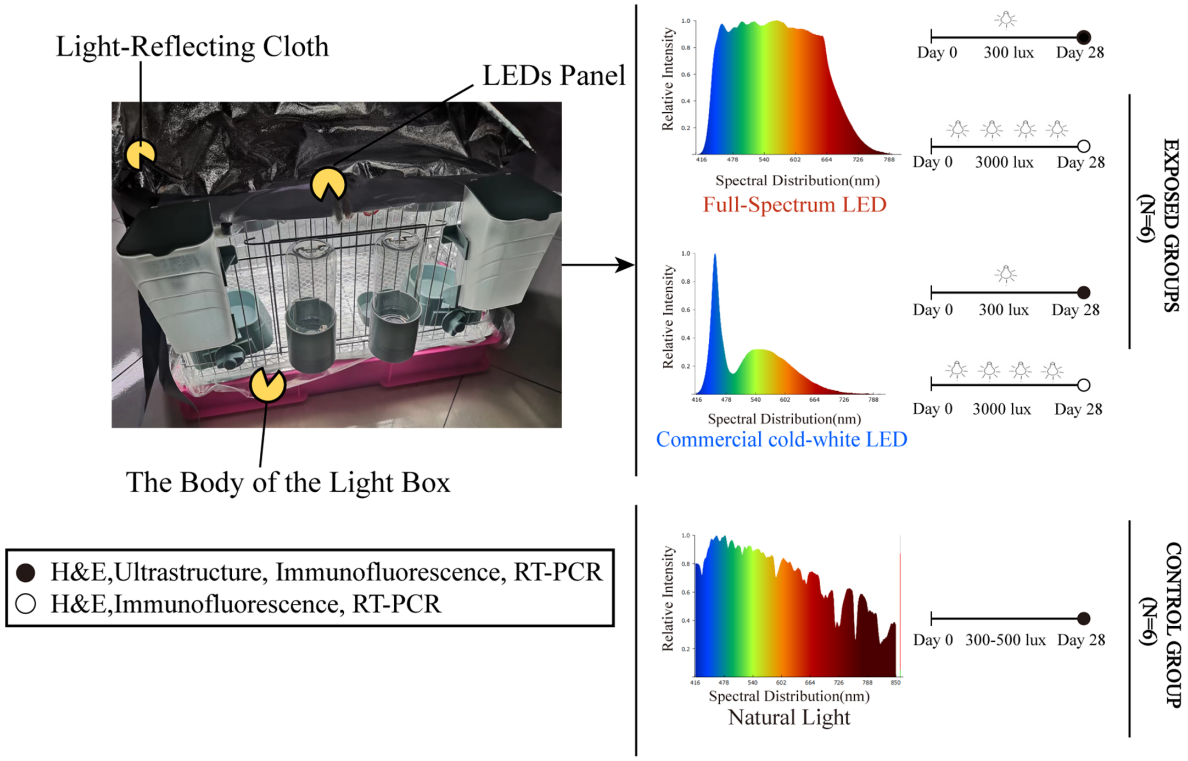

Figure 1. Experimental design of the study.

2.3 analysis system (Wuhan Servicebio) and quantified by averaging the values from 10 observation points in each image with Prism 8.0 (GraphPad Software, La Jolla, CA).

Transmission Electron Microscopy

Dorsal and ventral markings were made on the sclera, and several 1-mm3 tissue blocks were cut from dorsal and ventral retinas with 3% gluteraldehyde and 1.5% paraformaldehyde (4°C). The tissue underwent 1% osmic acid and 1.5% potassium ferrocyanide, followed by staining with 70% alcohol-saturated uranyl acetate. After dehydration, samples were then embedded in pure epoxy 618 embedding medium. Ultrathin sections were cut on an ultramicrotome (Leica UC-7; Leica, Wetzlar, Germany) at 90 nm and stained with uranyl acetate and lead citrate for 5 to 15 minutes. Samples were viewed and photographed using a Tecnai transmission electron microscope (FEI Company, Hillsboro, OR).

Immunofluorescence Staining

Immunofluorescence homologous double labeling was performed, and after the slides were deparaffinized and rehydrated they were immersed in ethylenediaminetetraacetic acid (EDTA) antigen retrieval buffer (pH 8.0). The objective tissues were covered with 3% bovine serum albumin (BSA) at room temperature for 30 minutes and incubated with antibody against S-opsin (rabbit anti-OPN1SW, 1:500; NOVUS Biologicals, Littleton, CO) overnight in a humid box at 4°C, washed in PBS the next day, and incubated with Alexa Fluor 488-conjugated goat anti-rabbit IgG (H+L) (1:400, Wuhan Servicebio) in the dark. Incubated slides with tyramide signal amplification–fluorescein isothiocyanate isomer (TSA-FITC; Wuhan Servicebio) solution for 10 minutes in dark conditions. Tissues were microwaved to remove antibodies and were incubated with the monoclonal antibody against GRP78/Bip (mouse anti-GRP78/Bip, 1:500; Bioss, Beijing, China) followed by Cy3 conjugated goat anti-mouse IgG (H+L) (1:300; Wuhan Servicebio) and 4′,6-diamidino-2-phenylindole (DAPI, 1:1000, 5min, Servicebio) to counterstain. Representative images were viewed and captured using Ortho-Fluorescent Microscopy (Nikon Eclipse C1; Nikon Instrument Inc., Tokyo, Japan). Aipathwell (Servicebio), a digital pathology image analysis software based on AI learning, was used to quantify the results and generate reports.

Real-Time Quantitative Polymerase Chain Reaction Analysis

We evaluated the effect of exposure to full-spectrum LEDs and commercial cold-white LEDs on the

Table. Primer Sequences for RT-qPCR Analysis

Gene	Sequence (5′→3′)	Length (bp)
S-opsin (*Cavia porcellus*)		
Forward	ATCGTAACCATGGGCTGGAC	20
Reverse	CATGGGCTTCCTACACACCA	20
GRP78/Bip (*Cavia porcellus*)		
Forward	TGGCATTCTTCGGGTGACAG	20
Reverse	AGTAGGCGTAGCTTTCCAGC	20
ATF4 (*Cavia porcellus*)		
Forward	GGCTGTGGATGAGTTGGTCA	20
Reverse	CATGTGTCATCCAACGTGGC	20
CHOP (*Cavia porcellus*)		
Forward	GAGCCCTCGGTCTCCAGATT	20
Reverse	CTGCTTGAGCCGTTCGTTCT	20
β-actin (*Cavia porcellus*)		
Forward	AGGACCTCTATGCCAACACAG	21
Reverse	CCAGGATAGAGCCGCCGA	18

expression of *S-opsin, GRP78/Bip, ATF4*, and *CHOP* mRNA in the retinas of albino guinea pigs. Individual intact retinas were isolated and homogenized using a rotor–stator homogenizer. The RNA in retinal tissues was extracted by TRIzol reagent (Sigma-Aldrich, St. Louis, MO). The expression of the target gene was detected by the 7500 Real-Time qPCR System (Applied Biosystems, Carlsbad, CA) with the Hieff qPCR SYBR Green Master Mix Kit (Yeasen Biotechnology Co., Ltd., Shanghai, China). Conditions for the real-time quantitative polymerase chain reaction (RT-qPCR) were as follows: 5 minutes at 95°C and then 10 seconds at 95°C, followed by two-step qPCR for 40 cycles consisting of 95°C for 15 seconds followed by 60°C for 35 seconds. The results are expressed relative to the β-actin internal control. The PCR primer sequences used are shown in the Table.

Statistical Analysis

Data conforming to the normal distribution were expressed as mean ± standard error of the mean. Statistical comparisons were performed with one-way ANOVA followed by Student's *t*-test or Dunnett's multiple comparison test using SPSS Statistics 23 (IBM Corporation, Chicago, IL) and GraphPad Prism 8.0. $P < 0.05$ was considered statistically significant.

Results

Less Retinal Morphological Damage from Full-Spectrum LEDs Than Commercial Cool-White LEDs

In the retinas, 10 layers of structures were intact and clear in the NC group (Fig. 2B). The nerve fibers in the optic nerve fiber layer were abundant and thick, limited internally by the inner limiting membrane. The cells in the ganglion cell layer (GCL) were large in size, aligned as a single layer of nuclei, intermixed with nerve fibers. The inner nuclear layer (INL) was clear and complete with the large and centrally cell core, and the outer nuclear layer (ONL) was formed of round or conical nuclei of photoreceptor cell bodies that included deeply stained rows of about four or five layers. The photoreceptor layer (inner and outer segment [IS/OS]) appeared as fibrillary striations with a thickness of about 22.67 ± 1.50 µm. The arrangement of the IS and OS is regularly arranged and relatively loose in albino guinea pigs; the RPE was found to be uniform in thickness, lacking pigment granules, and can be seen a small number of vacuoles.

After 28 days of light exposure at 300 lux, the structure and morphology of retinas in the FL-300 group were similar to those of the NC group (Fig. 2C). The thickness of the photoreceptor layer was 19.77 ± 1.31 µm with no statistical difference compared with the NC

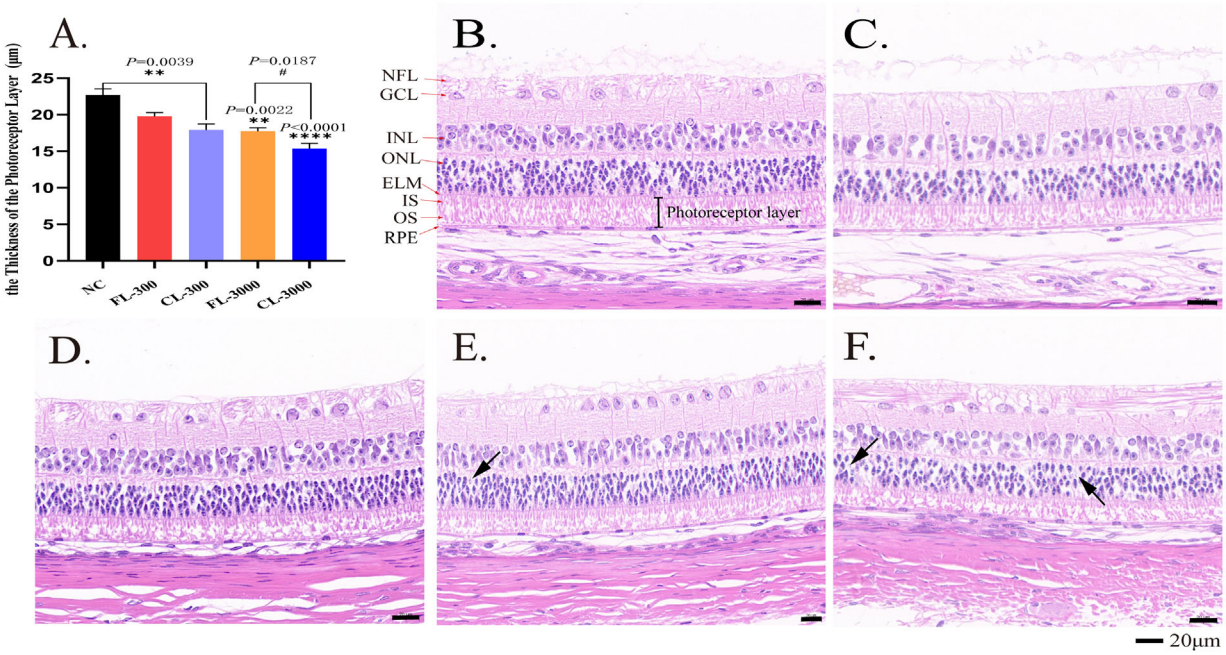

Figure 2. Effect of LEDs on the morphology of the retinas in albino guinea pigs after 28 days' exposure. (**A**) The thickness of the photoreceptor layer (IS and OS) in different groups. Representative retinal H&E stain results show retinal morphology of the NC group (**B**), FL-300 group (**C**), CL-300 group (**D**), FL-3000 group (**E**), and CL-3000 group (**F**). NFL, optic nerve fiber layer; GCL, ganglion cell layer; INL, inner nuclear layer; ONL, outer nuclear layer; IS, inner segments of the photoreceptor layer; OS, outer segments of the photoreceptor layer; ELM, external limiting membrane; RPE, retinal pigment epithelium. *Black arrows* identify the ghost cells. All data are expressed as the mean ± SD ($n > 3$). $^{**}P < 0.01$ and $^{****}P < 0.0001$ versus the NC group; $^{\#}P < 0.01$ versus the CL-3000 group. *Scale bar:* 20 μm.

group. In the retinas of the CL-300 group, the whole group had an overall thickness decrease in the photoreceptor layer, about 17.90 ± 2.07 μm, with an appearance of outer segment fragmentation and shorter inner segment (Fig. 2D), which had a statistical difference compared with the NC group ($P = 0.0039$).

At 3000-lux intensity, we found a greater degree of photoreceptor layer damage in two LED-exposed groups with drastic morphological changes of the OS and IS, including condensed ISs and overall disorganization of OSs. The ONL in the CL-3000 group showed apparent spacing between the cell bodies, with some pyknotic nuclei and ghost cells (black arrows) (Figs. 2E, 2F), as compared to the FL-3000 group, which had relatively neater ISs (Fig. 2E). Meanwhile, the nerve fiber layer displayed exudation and irregular lines in both LED-exposed groups under 3000 lux (Figs. 2E, 2F). The thickness of the photoreceptor layers in the two groups were 17.74 ± 1.27 μm and 15.37 ± 1.93 μm, which both had statistically significant differences compared with the NC group ($P = 0.0022$ and $P < 0.0001$, respectively). In addition, photoreceptor layers of the CL-3000 group decreased significantly as compared with the FL-3000 group ($P = 0.0187$) (Fig. 2A). The data presented here suggest that LED exposure with intensities of 3000 lux for 4 weeks can induce severe retinal morphological damage in albino guinea pigs, but it is apparent that the damage caused by the full-spectrum LEDs was significantly attenuated compared with that caused by the commercial cold-white LEDs.

Ultrastructure Allowed a More Detailed Comparison of the Retinal Morphological Damage Caused by LEDs at 300 Lux

Transmission electron microscopy (TEM) was used to observe more detailed morphological changes in the retinas of the NC group, the FL-300 group, and the CL-300 group. We examined the ultrastructure of OS, ONL, and mitochondria or ER in both the ventral and dorsal retina. In the NC group, the OSs in the dorsal and ventral retina were neat and contained well-organized and horizontally aligned membranous discs (Figs. 3A, 3D); lysosomes were seen around them, indicating an active metabolism (Fig. 3D, yellow arrows). The OS in the dorsal region was typically arranged densely and neatly in both the FL-300 and CL-300 groups (Figs. 3B, 3C). The membranous discs of the OS in the ventral retina showed mild malalignment and reduced size in the

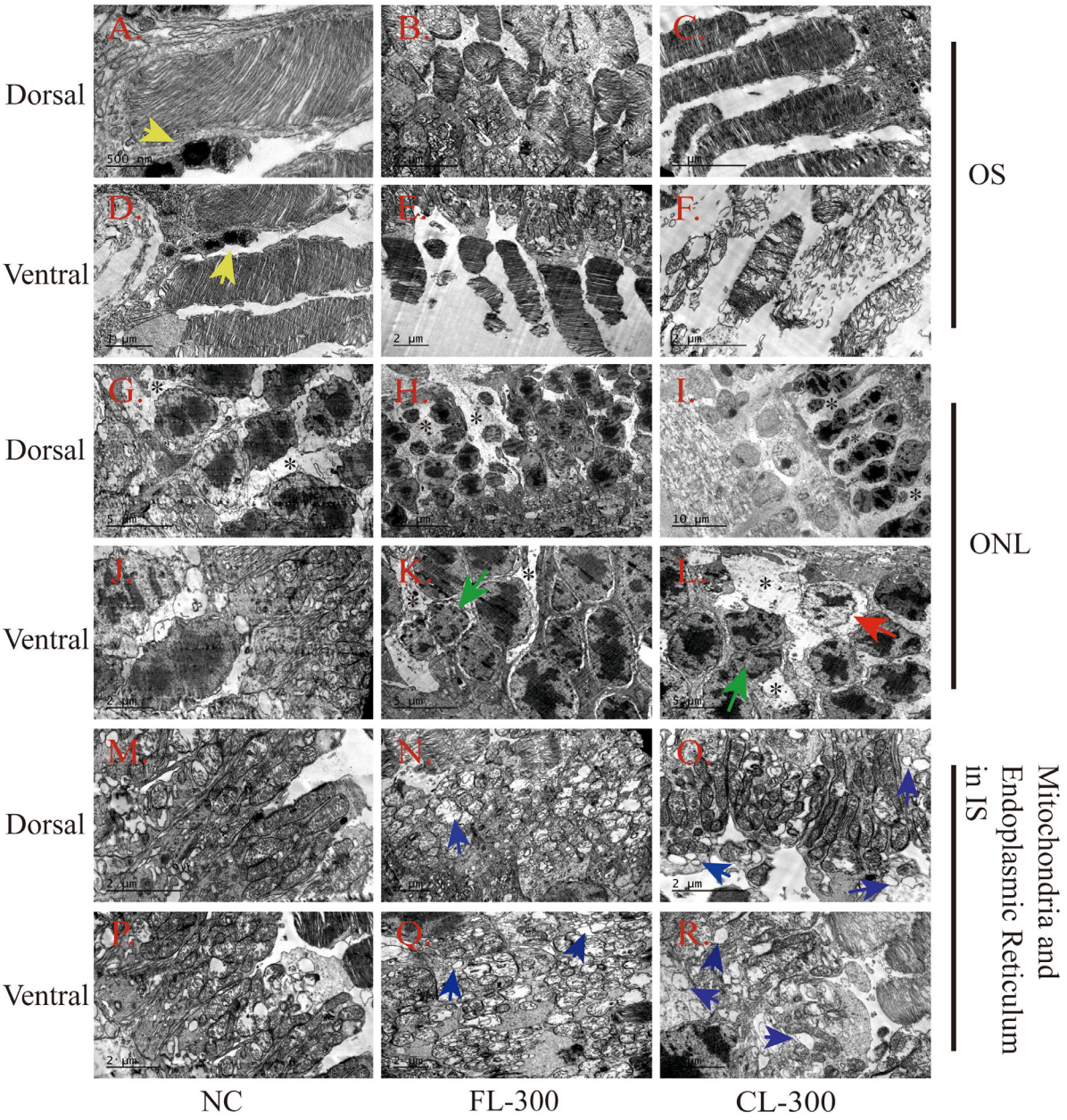

Figure 3. Representative TEM images of the retina in albino guinea pigs after 28 days of exposure at 300 lux. (**A**, **D**) The OS from the dorsal and ventral regions, respectively, in the NC group. *Scale bars*: 500 nm and 1 µm, respectively. (**B**, **E**) The OS from the dorsal and ventral regions, respectively, in the FL-300 group. *Scale bars*: 5 µm and 2 µm, respectively. (**C**, **F**) The OS from the dorsal and ventral regions, respectively, in the CL-300 group. *Scale bars*: 2 µm. (**G**, **J**) The ONL from the dorsal and ventral regions, respectively, in the NC group. *Scale bars*: 5 µm and 2 µm, respectively. (**H**, **K**) The ONL from the dorsal and ventral regions, respectively, in the FL-300 group. *Scale bars*: 10 µm and 5 µm, respectively. (**I**, **L**) The ONL from the dorsal and ventral regions, respectively, in the CL-300 group. *Scale bars*: 10 µm and 5 µm, respectively. (**M**, **P**) The mitochondria and ER from the dorsal and ventral regions, respectively, in the NC group. *Scale bars*: 2 µm. (**N**, **Q**) The mitochondria and ER from the dorsal and ventral regions, respectively, in the FL-300 group. *Scale bars*: 2 µm. (**O**, **R**) The mitochondria and ER from the dorsal and ventral regions, respectively, in the CL-300 group. *Scale bars*: 2 µm. *Yellow arrows* identify the lysosomes; *green arrows* identify the edge aggregation of chromatin; the *red arrow* identifies the appearance of a widening of the perinuclear space; *blue arrows* identify the expanded ERs; and *black asterisks* identify the Müller cell processes.

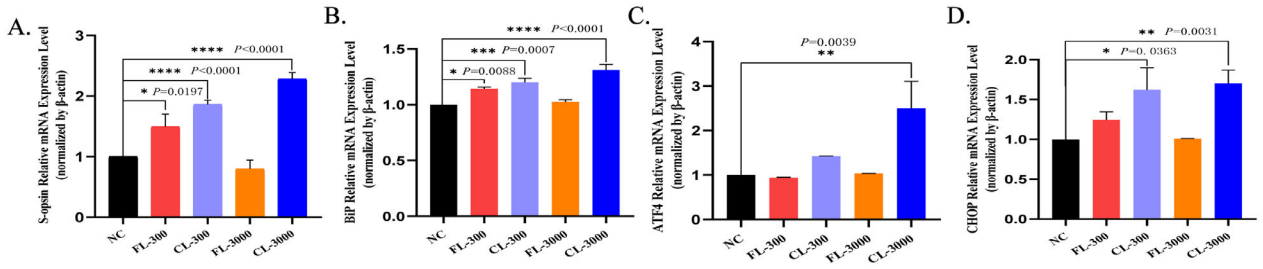

Figure 4. Figures show mRNA expression of the retinas of unilluminated albino guinea pigs and albino guinea pigs exposed to full-spectrum LEDs (FL) and commercial cold-white LEDs (CL) for 28 days tested via RT-qPCR. (**A**) S-opsin, (**B**) GRP78/Bip, (**C**) ATF4, (**D**) CHOP. The values shown are mean ± SD analyzed with one-way ANOVA ($n > 3$). $^{*}P < 0.05$, $^{**}P < 0.01$, $^{***}P < 0.001$, and $^{****}P < 0.0001$ versus the NC group.

FL-300 group (Fig. 3E). There was significant disorganization of the membranous discs in the ventral retina in the CL-300 group (Fig. 3F). The cells in the ONL were uniform in size in the NC group, and the chromatin in the center of the nucleus was deeply stained (Figs. 3G, 3J). In the retinas of the LED-exposed groups, Müller cell processes (black asterisks) appeared in the space between photoreceptor somas and became electron lucent and more loosely distributed (Figs. 3G–3I, 3K, 3L). Edge aggregation of chromatin (green arrows) occurred in the ventral retinas, indicating cell degeneration in the FL-300 and CL-300 groups (Figs. 3K, 3L), and the CL-300 group even exhibited local widening of the perinuclear space (Fig. 3L, red arrow).

Longitudinal tubular mitochondria and abundant rough endoplasmic reticulum can be seen in the ISs of the photoreceptors (Figs. 3M, 3P). Under the LED lighting, intensive mitochondria appeared with edema, vacuolization changes, and breaks of mitochondrial cristae. Moreover, massive expanded ERs were seen (Figs. 3N, 3O, 3Q, 3R, blue arrows). Overall, morphological damage was less severe in the dorsal region than the ventral, possibly due to the continuous production of S-opsin in the ventral retina induced by the blue light in the LEDs; S-opsin is not readily degraded and induced the expression of ER stress.[25]

Commercial Cold-White LED Increased the Expression of S-Opsin and ER Stress-Related Factors in Retinas of Guinea Pigs

It has been reported that excessive light exposure causes S-opsin aggregation and leads to ER stress in the cone photoreceptor-derived cell line 661W.[26] To investigate further whether in vivo exposure to commercial cold-white LEDs and full-spectrum LEDs affects the expression of genes related to the ER stress response, we performed RT-qPCR using primers specific for S-opsin: GRP78/Bip, ATF4, and CHOP mRNA. The RT-qPCR showed that the full-spectrum LEDs resulted in only a significant but mild increase of S-opsin and GRP78/Bip mRNA ($P < 0.05$) at 300 lux (Figs. 4A, 4B), but mRNA expression was not significant under exposure to FL-3000. As expected, the commercial cold-white LEDs caused a significant increase of S-opsin, GRP78/Bip, and CHOP mRNA expression under both 300 lux and 3000 lux and a marked increase of ATF4 mRNA at 3000 lux (Fig. 4).

Based on the immunofluorescence results, Aipathwell revealed that S-opsin was predominantly expressed in specific cellular layers of the retina. In the normal retina, weak punctuate labeling of S-opsin was seen in the outer plexiform layer (OPL) and photoreceptor layer. Moreover, the immunoreactivity of GRP78/Bip was observed in the GCL, INL, OPL, and IS. It has been reported that the GRP78/Bip is mainly localized in thin cytoplasmic components within the intercellular spaces, which might be process of Müller glial cells.[27] Moreover, they were distributed throughout the nuclear membrane and might be the ER (Fig. 5A). Compared to the control group, S-opsin expression upregulated by the CL was mainly located in the inner plexiform layer, OPL, IS, and OS. Strong immunoreactivity of GRP78/Bip (used as an ER marker)[28] in the CL-exposed groups was observed in the cytoplasmic component of the intercellular spaces of INL and ONL, which appeared as circles and thick irregular lines. They gathered in the IS and migrated to the OS, where the merge of GRP78/Bip and S-opsin occurred (Figs. 5C, 5E, white arrows). It has been suggested that Müller cell processes may become hypertrophied, migrate to the damaged area, and continue to proliferate to new photoreceptors. This is consistent with the characteristics of photoreceptor degeneration in adult zebrafish,[10] a classic animal model of LIRD.

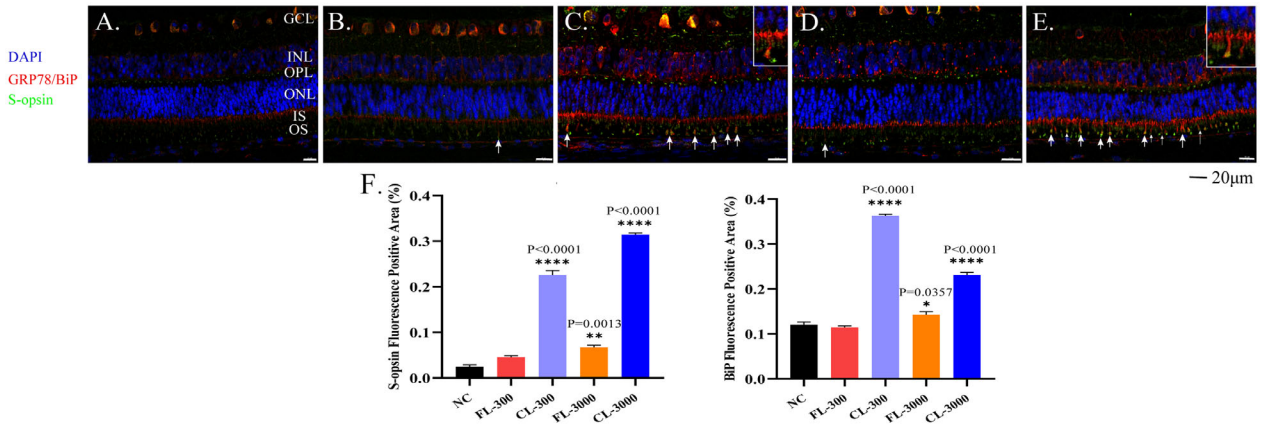

Figure 5. Immunofluorescence of retinas showed the expression levels of S-opsin and GRP78/Bip. (**A**) NC group; (**B**) FL-300 group; (**C**) CL-300 group; (**D**) FL-3000 group; (E) CL-3000 group. Retinas were stained with antibodies against S-opsin (*green*) and M-opsin (*red*). Nuclei were stained with DAPI (*blue*). In the experimental groups, GRP78/Bip and S-opsin aggregation is indicated by *white arrows* with magnified details in **C** and **E**. (**F**) Expression levels in S-opsin and GRP78/Bip quantified by Aipathwell show positive fluorescence areas in the retinas. The values shown are mean ± SD analyzed with one-way ANOVA ($n > 3$). $^{*}P < 0.05$, $^{**}P < 0.01$ and $^{****}P < 0.0001$ versus the NC group. *Scale bar*: 20 μm.

Retinas exposed to the CL experienced a merge of GRP78/Bip and S-opsin in the OS at either 300 lux or 3000 lux, whereas there was a significant but mild increase of GRP78/Bip and S-opsin protein only in the FL-3000 group (Figs. 5B, 5D, white arrows). The Aipathwell quantified the results by dividing the positive fluorescence area by the total area,[29] which further proved that S-opsin and GRP78/Bip expressions increased significantly after exposure to the commercial cold-white LEDs (Fig. 5F). These results indicate that the light toxicity of full-spectrum LEDs is less than that of commercial cold-white LEDs even under a high illuminance and that commercial cold-white LEDs can induce intense ER stress at low illuminance of 300 lux.

Discussion

Commercial cold-white LEDs use a large amount of blue light to emit the white light which is reportedly harmful to the eye,[22] especially with regard to LIRD. LIRD is known to play essential roles in many retinal diseases, including macular degeneration and retinal dystrophy.[10] In our study, when a spectrometer was used to compare the commercial cold-white and full-spectrum LEDs, the full-spectrum LEDs has almost no gap in the visible light spectrum (Fig. 1), which converts most of the blue light into blue–green light.[30] This may solve the problem of the blue light hazard presented by commercial cold-white LEDs,[31] and a few studies are comparing the effects of these two different spectral LEDs on LIRD.

LIRD is extensively used in zebrafish or rodents to affect the photoreceptors[32,33] and has been used in an albino background,[34–36] which is very susceptible to LIRD, because albino animals lack melanin in the RPE, which absorbs light passing through the retina. Nevertheless, few experiments have been conducted to analyze LIRD in albino guinea pigs. Here, we successfully described a LIRD model in albino guinea pigs that resulted in varying degrees of damage to photoreceptor layers (IS and OS) resulting from exposure to two LEDs with different spectrums.

The Standard for Lighting Design of Buildings issued by the Ministry of Housing and Urban-Rural Development of the People's Republic of China[37] pointed out that the standard light illuminance for writing indoors is 300 lux. Also, the greater the illuminance, the higher the radiation of the spectrum.[38] Referring to the illuminance grading standard, we prepared two types of light illuminance: 300 lux, which is close to usual domestic light use, and 3000 lux, which reflects extreme exposure. The other parameters of the light were kept consistent as far as possible.

Reduction of the photoreceptor layer has been previously described in rat models of LIRD, such as F344/N rats and albino Sprague Dawley rats.[39,40] In our study, as expected, at high illuminance (i.e., 3000 lux), a significant reduction of photoreceptor layer thickness was found in two experimental groups, especially in the CL-3000 group, which had a lower thickness and the appearance of disordered and sparse photoreceptor segments all over the retina. At standard

writing illuminance (i.e., 300 lux), retinal damage was observed in the CL-300 group, which induced a statistical reduction in the thickness of the photoreceptor layer. In contrast, the FL-300 group did not differ compared to the photoreceptor layer thickness in the NC group.

Before this study, studies have reported that rod OSs and ISs undergo ultrastructural changes induced by light in a transgenic *Xenopus* modal.[41] Here, TEM showed that the OS in the ventral region was severely broken and more diffuse compared to the dorsal retina. Meanwhile, edge aggregation of chromatin and a widening of the perinuclear space revealed the death of cells induced by light toxicity. It is important to note that, in retinal ultrastructure, at the 300 lux illuminance, we could disintegration, disconnection, and cavitation of the ER; extensive vesiculation adjacent to the ER; and mitochondrial swelling and cristae shortening, diminishing, or even disappearing, all of which indicated cell degeneration.[42] These morphological findings, including H&E and TEM, correspond with the suggestion of Behar-Cohen et al.,[16] who previously suspected that commercial cold-white LEDs may cause retinal toxicity even under occupational domestic illuminance conditions, as well as extreme conditions.

Guinea pigs have two types of opsins,[43] including medium-wavelength opsins (M-opsin), which is predominantly dorsal, and S-opsin, which is predominantly ventral.[44] The changes here due to LIRD may relate to the production of S-opsin mainly distributed in the ventral retina.[45,46] It has been reported that M-opsin is easily degraded, but degradation of excessive light-induced S-opsin by the proteasome is difficult and in turn induces the aggregation of S-opsin and occurrence of ER stress.[46–48]

ER stress is a response process in which cells activate a series of signaling pathways in response to conditions such as the accumulation of misfolded and unfolded protein and the dysregulation of calcium homeostasis, which have been observed in neurodegenerative diseases such as Parkinson's disease, Alzheimer's disease, and so on.[49–51] GRP78/Bip protein is considered to be the primary sensor and master regulator of he ER stress; it is localized to membranous structures and is seen on the nuclear membrane and ER in retinal neurons and glial cells at the subcellular level.[52,53] As an ER chaperone, GRP78/Bip overexpression can indicate occurrence of the unfolded protein response (UPR), which maintains protein homeostasis and promotes cell survival.[54] However, ER stress can be prolonged and induce ER stress-induced apoptosis if the UPR fails to recover ER function.[55,56] ATF4, a downstream molecule of the ER protein sensor PERK, is an essential mediator of ER stress-induced apoptosis[57]; and CHOP is a crucial member of the enhancer-binding protein family induced by ER stress and can be elevated by the PERK-ATF4 pathway to mediate apoptosis.[58] Changes in the expression levels of both may indicate ER stress.

In this research, we found an increase in the mRNA and protein levels of S-opsin and GRP78/Bip by RT-qPCR and immunofluorescence in retinas after LED exposure for 28 days, especially under CL exposure at 3000 lux. Furthermore, ATF4 and CHOP were markedly upregulated in CL-exposed albino guinea pigs' retinas. This suggests that overexposure to CLs induce the aggregation of S-opsin and severe UPR, which lead to cell death. This finding suggests that ER stress plays a vital role in LIRD.

Immunofluorescence detected strong GRP78/BiP immunoreactivity in the INL in addition to the ONL, which is consistent with a report by Yang et al.,[59] which suggests that the UPR may also occur in the inner retina during LIRD. GRP78/BiP can also prompt the process of Müller cells, which are responsible for the retinal metabolism through the UPR, as shown in diabetic retinopathy.[60,61] Also, the activation and migration of Müller cells in LIRD have been confirmed to modulate the apoptotic loss of photoreceptor cells in the outer retina.[62] TEM in the present work also revealed that broadened Müller cell processes intervened in the space between photoreceptor somas, indicating metabolic modulation in the degenerative retina and engulfing and clearing of the damaged photoreceptor.

Interestingly, we found that the FL-300 exposure increased the mRNA expression levels in S-opsin and GRP78/BiP, whereas the expression went back to normal when the illuminance reached 3000 lux. This result may support the idea that the UPR includes two phases[28]: early UPR, which can suppress ER stress and restore ER homeostasis, and late UPR, which is too severe to restore ER homeostasis and leads to apoptotic cell death.[27] In the initial exposure stage, the retinas experience external stress during early UPR, but the ER stress cannot restore ER homeostasis, probably due to the intense blue light toxicity in the CL that causes cell apoptosis.

Photodamage by light is affected by various factors, including not only the spectral distribution and illuminance but also the color rendering, irradiance, correlated color temperature, visible light wavelength, and exposure time, among other factors.[63] For example, the relative intensity of red light in the full-spectrum LED has also increased, and the benefits of red light in treating diseases and preventing myopia have been confirmed in many studies.[64,65] We will further investigate this aspect in a follow-up study.

Because LEDs are becoming the predominant light source in our domestic environment, the biological effects on the eyes must be clarified, and it becomes urgent to develop a more comprehensive and detailed understanding of their biological effects. Here, an important finding was that spectral distribution plays a vital role in the development of LIRD in albino guinea pigs and relates to the S-opsin aggregation and ER stress. Full-spectrum LEDs with a reduced relative intensity of blue light still induced morphological retinal degeneration. Irrespective of the illuminance (300 lux or 3000 lux), the alterations presented in the FL-exposed groups were progressive and aggravated in the CL-exposed groups, especially in the photoreceptor layer.

In conclusion, this study suggests that full-spectrum LEDs offer specific eye protection and eye adaptability and can well replace commercial cold-white LEDs in both clinical practice and research.

Acknowledgments

The authors thank Yan Huang, PhD, for her critical reading of the manuscript and Sungoing Optoelectronics Technology Co., Ltd., for its apparatus help.

Disclosure: **W. Chen**, None; **R. Lin**, None; **K. Xiao**, None; **K. Yuan**, None; **Z. Chen**, None; **Y. Huang**, None

References

1. Roberts J. Update on the positive effects of light in humans. *Photochem Photobiol*. 2005;81(3):490–492.
2. Nakano T, Chiang K, Chen C, et al. Sunlight exposure and phototherapy: perspectives for healthy aging in an era of COVID-19. *Int J Environ Res Public Health*. 2021;18(20):10950.
3. Huang P, Hsiao Y, Tsai C, et al. Protective behaviours of near work and time outdoors in myopia prevalence and progression in myopic children: a 2-year prospective population study. *Br J Ophthalmol*. 2020;104(7):956–961.
4. Shang Y, Wang G, Sliney D, Yang C-H, Lee L-L. White light-emitting diodes (LEDs) at domestic lighting levels and retinal injury in a rat model. *Environ Health Perspect*. 2014;122(3):269–276.
5. Marshall J. Light in man's environment. *Eye (Lond)*. 2016;30(2):211–214.
6. Lin C, Yang C-M, Yang C-H. Protective effect of astaxanthin on blue light light-emitting diode-induced retinal cell damage via free radical scavenging and activation of PI3K/Akt/Nrf2 pathway in 661W cell model. *Mar Drugs*. 2020;18(8):387.
7. Ouyang X, Yang J, Hong Z, Wu Y, Xie Y, Wang G. Mechanisms of blue light-induced eye hazard and protective measures: a review. *Biomed Pharmacother*. 2020;130:110577.
8. Zhao Z, Zhou Y, Tan G, Li J. Research progress about the effect and prevention of blue light on eyes. *Int J Ophthalmol*. 2018;11(12):1999–2003.
9. Tang W, Guo J, Liu W, Xu G. Ferrostatin-1 attenuates ferroptosis and protects the retina against light-induced retinal degeneration. *Biochem Biophys Res Commun*. 2021;548:27–34.
10. Thomas JL, Thummel R. A novel light damage paradigm for use in retinal regeneration studies in adult zebrafish. *J Vis Exp*. 2013(80):e51017.
11. Chan P, Stolz J, Kohl S, Chiang W-C, Lin JH. Endoplasmic reticulum stress in human photoreceptor diseases. *Brain Res*. 2016;1648:538–541.
12. Ooe E, Tsuruma K, Kuse Y, Kobayashi S, Shimazawa M, Hara H. The involvement of ATF4 and S-opsin in retinal photoreceptor cell damage induced by blue LED light. *Mol Vis*. 2017;23:52–59.
13. Ooe E, Kuse Y, Yako T, et al. Bilberry extract and anthocyanins suppress unfolded protein response induced by exposure to blue LED light of cells in photoreceptor cell line. *Mol Vis*. 2018;24:621–632.
14. Ostrin L. Ocular and systemic melatonin and the influence of light exposure. *Clin Exp Optom*. 2019;102(2):99–108.
15. Zhang N, Wang Z, Zhao J, et al. Improving CRI and luminous efficiency of phosphor-converted full-spectrum WLEDs by powder sedimentation packaging. *ACS Appl Electron Mater*. 2021;3(3):1115–1126.
16. Behar-Cohen F, Martinsons C, Viénot F, et al. Light-emitting diodes (LED) for domestic lighting: any risks for the eye? *Prog Retin Eye Res*. 2011;30(4):239–257.
17. Austin E, Geisler A, Nguyen J, et al. Visible light. Part I: properties and cutaneous effects of visible light. *J Am Acad Dermatol*. 2021;84(5):1219–1231.
18. Najjar RP, De La Barca JMC, Barathi VA, et al. Ocular growth and metabolomics are dependent upon the spectral content of ambient white light. *Sci Rep*. 2021;11(1):7586.
19. Muralidharan A, Low S, Lee Y, et al. Recovery from form-deprivation myopia in chicks is dependent upon the fullness and correlated color temperature of the light spectrum. *Invest Ophthalmol Vis Sci*. 2022;63(2):16.

20. Wang M, Schaeffel F, Jiang B, et al. Effects of light of different spectral composition on refractive development and retinal dopamine in chicks. *Invest Ophthalmol Vis Sci*. 2018;59(11):4413–4424.
21. Chen W, Xiao K, Lin R, et al. Effect of light-emitting diodes with different color rendering indexes on the ocular tissues of rat. *Int J Ophthalmol*. 2022;15(7):1035–1043.
22. Krigel A, Berdugo M, Picard E, et al. Light-induced retinal damage using different light sources, protocols and rat strains reveals LED phototoxicity. *Neuroscience*. 2016;339:296–307.
23. Lin J. Solar spectral LED eye protection flat lamp[P]. China:ZL201210136847.3, 2015-10-21.
24. Yu Z, Qiu S, Chen X, et al. Neuroglobin - a potential biological marker of retinal damage induced by LED light. *Neuroscience*. 2014;270:158–167.
25. Zhang T, Zhang N, Baehr W, Fu Y. Cone opsin determines the time course of cone photoreceptor degeneration in Leber congenital amaurosis. *Proc Natl Acad Sci USA*. 2011;108(21):8879–8884.
26. Kuse Y, Ogawa K, Tsuruma K, Shimazawa M, Hara H. Damage of photoreceptor-derived cells in culture induced by light emitting diode-derived blue light. *Sci Rep*. 2014;4:5223.
27. Park Y, Kim H, Lee S, Zhang Y, Kim I-B. Expression of the endoplasmic reticulum stress marker GRP78 in the normal retina and retinal degeneration induced by blue LED stimuli in mice. *Cells*. 2021;10(5):995.
28. Nakanishi T, Shimazawa M, Sugitani S, et al. Role of endoplasmic reticulum stress in light-induced photoreceptor degeneration in mice. *J Neurochem*. 2013;125(1):111–124.
29. Luo W, Ai L, Wang B, Zhou Y. High glucose inhibits myogenesis and induces insulin resistance by down-regulating AKT signaling. *Biomed Pharmacother*. 2019;120:109498.
30. Mondal K, Pramanik A, Mondal T, Panja SS, Sarkar R, Kumbhakar P. Self-assembly of solvent-stabilized au nanocluster as efficient Förster resonance energy-transfer initiator for white light generation. *J Phys Chem Lett*. 2022;13(13):3079–3088.
31. Lee S, Matsumori K, Nishimura K, et al. Melatonin suppression and sleepiness in children exposed to blue-enriched white LED lighting at night. *Physiol Rep*. 2018;6(24):e13942.
32. Kikuchi Y, Sugano E, Yuki S, et al. SIG-1451, a novel, non-steroidal anti-inflammatory compound, attenuates light-induced photoreceptor degeneration by affecting the inflammatory process. *Int J Mol Sci*. 2022;23(15):8802.
33. Cheng K, Hsu Y, Liu W, et al. The role of oxidative stress and autophagy in blue-light-induced damage to the retinal pigment epithelium in zebrafish in vitro and in vivo. *Int J Mol Sci*. 2021;22(3):1338.
34. Yamashita H, Hoenerhoff M, Peddada S, Sills RC, Pandiri AR. Chemical exacerbation of light-induced retinal degeneration in F344/N rats in national toxicology program rodent bioassays. *Toxicol Pathol*. 2016;44(6):892–903.
35. Novikova Y, Gancharova O, Eichler O, Philippov PP, Grigoryan EN. Preventive and therapeutic effects of SkQ1-containing Visomitin eye drops against light-induced retinal degeneration. *Biochemistry (Mosc)*. 2014;79(10):1101–1110.
36. Shibuya K, Tomohiro M, Sasaki S, Otake S, et al. Characteristics of structures and lesions of the eye in laboratory animals used in toxicity studies. *J Toxicol Pathol*. 2015;28(4):181–188.
37. Ministry of Housing and Urban-Rural Development of the People's Republic of China. Standard for Lighting Design of Buildings: GB 50034-2013. Beijing, China: Ministry of Housing and Urban-Rural Development of the People's Republic of China; 2013.
38. Rucker F. Monochromatic and white light and the regulation of eye growth. *Exp Eye Res*. 2019;184:172–182.
39. Yamashita H, Hoenerhoff M, Shockley K, et al. Reduced disc shedding and phagocytosis of photoreceptor outer segment contributes to kava kava extract-induced retinal degeneration in F344/N rats. *Toxicol Pathol*. 2018;46(5):564–573.
40. Brandli A, Johnstone D, Stone J. Remote ischemic preconditioning protects retinal photoreceptors: evidence from a rat model of light-induced photoreceptor degeneration. *Invest Ophthalmol Vis Sci*. 2016;57(13):5302–5313.
41. Bogéa T, Wen R, Moritz O. Light induces ultrastructural changes in rod outer and inner segments, including autophagy, in a transgenic *Xenopus laevis* P23H rhodopsin model of retinitis pigmentosa. *Invest Ophthalmol Vis Sci*. 2015;56(13):7947–7955.
42. Agrawal SA, Burgoyne T, Eblimit A, et al. REEP6 deficiency leads to retinal degeneration through disruption of ER homeostasis and protein trafficking. *Hum Mol Genet*. 2017;26(14):2667–2677.
43. Zou L, Zhu X, Liu R, et al. Effect of altered retinal cones/opsins on refractive development under monochromatic lights in guinea pigs. *J Ophthalmol*. 2018;2018:9197631.
44. Applebury ML, Antoch MP, Baxter LC, et al. The murine cone photoreceptor: a single cone type expresses both S and M opsins with retinal spatial patterning. *Neuron*. 2000;27(3):513–523.

45. Rhim I, Coello-Reyes G, Ko H-K, et al. Maps of cone opsin input to mouse V1 and higher visual areas. *J Neurophysiol*. 2017;117(4):1674–1682.
46. Xu H, Enemchukwu N, Zhong X, Zhang O, Fu Y. Deletion of M-opsin prevents M cone degeneration in a mouse model of Leber congenital amaurosis. *Am J Pathol*. 2020;190(5):1059–1067.
47. Zhang T, Enemchukwu NO, Jones A, et al. Genetic deletion of S-opsin prevents rapid cone degeneration in a mouse model of Leber congenital amaurosis. *Hum Mol Genet*. 2015;24(6):1755–1763.
48. Fan B, Zhang CX, Chi J, et al. The molecular mechanism of retina light injury focusing on damage from short wavelength light. *Oxid Med Cell Longev*. 2022;2022:8482149.
49. Yasmeen N, Datta M, Kumar V, Alshehri FS, Almalki AH, Haque S. Deciphering the link between ER signaling and microRNA in pathogenesis of Alzheimer's disease. *Front Aging Neurosci*. 2022;14:880167.
50. Smith L, Schapira A. GBA variants and Parkinson disease: mechanisms and treatments. *Cells*. 2022;11(8):1261.
51. Wodrich A, Scott A, Shukla A, Harris BT, Giniger E. The unfolded protein responses in health, aging, and neurodegeneration: recent advances and future considerations. *Front Mol Neurosci*. 2022;15:831116.
52. Mohlin C, Taylor L, Ghosh F, Johansson K. Autophagy and ER-stress contribute to photoreceptor degeneration in cultured adult porcine retina. *Brain Res*. 2014;1585:167–183.
53. Wu B, Zhao TV, Jin K, et al. Mitochondrial aspartate regulates TNF biogenesis and autoimmune tissue inflammation. *Nat Immunol*. 2021;22(12):1551–1562.
54. Bertolotti A, Zhang Y, Hendershot LM, Harding HP, Ron D, et al. Dynamic interaction of BiP and ER stress transducers in the unfolded-protein response. *Nat Cell Biol*. 2000;2(6):326–332.
55. Hetz C, Papa F. The unfolded protein response and cell fate control. *Mol Cell*. 2018;69(2):169–181.
56. Gao H, He C, Hua R, et al. Endoplasmic reticulum stress of gut enterocyte and intestinal diseases. *Front Mol Biosci*. 2022;9:817392.
57. Pitale P, Gorbatyuk O, Gorbatyuk M. Neurodegeneration: keeping ATF4 on a tight leash. *Front Cell Sci*. 2017;11:410.
58. Turpin J, El-Safadi D, Lebeau G, et al. CHOP pro-apoptotic transcriptional program in response to ER stress is hacked by Zika virus. *Int J Mol Sci*. 2021;22(7):3750.
59. Yang L-P, Wu L-M, Guo X-J, Li Y, Tso MOM. Endoplasmic reticulum stress is activated in light-induced retinal degeneration. *J Neurosci Res*. 2008;86(4):910–919.
60. Kelly K, Wang J, Zhang S. The unfolded protein response signaling and retinal Müller cell metabolism. *Neural Regen Res*. 2018;13(11):1861–1870.
61. Chalour N, Maoui A, Rat P, et al. AβPP-induced UPR transcriptomic signature of glial cells to oxidative stress as an adaptive mechanism to preserve cell function and survival. *Curr Alzheimer Res*. 2018;15(7):643–654.
62. Rutar M, Natoli R, Chia R, Valter K, Provis JM. Chemokine-mediated inflammation in the degenerating retina is coordinated by Müller cells, activated microglia, and retinal pigment epithelium. *J Neuroinflammation*. 2015;12:8.
63. Yoon H, Taylor C, Rucker F. Spectral composition of artificial illuminants and their effect on eye growth in chicks. *Exp Eye Res*. 2021;207:108602.
64. Hung L, Arumugam B, She Z, Ostrin L, Smith EL III. Narrow-band, long-wavelength lighting promotes hyperopia and retards vision-induced myopia in infant rhesus monkeys. *Exp Eye Res*. 2018;176:147–160.
65. Rohringer S, Holnthoner W, Chaudary S, et al. The impact of wavelengths of LED light-therapy on endothelial cells. *Sci Rep*. 2017;7(1):10700.